Experimental Thermal and Fluid Science xxx (2012) xxx–xxx

Contents lists available at SciVerse ScienceDirect

Experimental Thermal and Fluid Science

journal homepage: www.elsevier.com/locate/etfs

Drag reduction effect of nanobubble mixture flows through micro-orifices and capillaries

Akiomi Ushida [a,*], Tomiichi Hasegawa [b], Toshiyuki Nakajima [c], Hiroshige Uchiyama [d], Takatsune Narumi [b]

[a] Center of Fostering Innovative Leadership, Niigata University, Japan
[b] Faculty of Engineering, Niigata University, Japan
[c] Diako Engineering Company, Ltd., Japan
[d] Graduate School of Science and Technology, Niigata University, Japan

ARTICLE INFO

Article history:
Received 12 April 2011
Received in revised form 15 November 2011
Accepted 7 January 2012
Available online xxxx

Keywords:
Nanobubble
Pressure drop
Orifice
Capillary
Drag reduction

ABSTRACT

Much research on microbubbles and their drag reduction effect has been reported. However, few studies have focused on nanobubbles, which have sub-micrometer size. Mixtures of surfactants and polymers are known to reduce drag, but their use is limited because of environmental concerns. In this research, nanobubble mixtures for water and glycerol were passed through several sizes of micro-orifices and capillaries, and the resultant pressure drops, as compared with water and glycerol, were evaluated. For a small orifice (≤50 μm) and capillary (≤70 μm), the experimentally observed pressure drop was less than that for water. This phenomenon is considered in terms of interface behavior and attributed to the electrical interaction between an electric double layer and nanobubbles. The results of the present research suggest that the addition of nanobubbles to a liquid results in excellent drag reduction.

1. Introduction

In recent years, copious research into microbubbles has been carried out from the perspectives of drag reduction, cleaning, and purification. Kodama et al. [1] reported on the reduced friction that acts upon the outside of ships' hulls as a result of microbubbles. Also, Kato et al. [2] reported that as the density of microbubbles in a turbulent boundary layer is increased, the intensity of turbulence in the buffer layer is reduced. Liu et al. [3,4] reported that the quantity of coagulant used in the treatment of dye wastewater can be reduced by using microbubbles. The use of nanobubbles, which are bubbles having sub-micrometer size, has been reported in the field of microelectromechanical systems for washing semiconductors [5], but there have been no reports of nanobubbles being used in other applications, because the flow properties and washing effects of nanobubbles are not yet well understood. Burger et al. [6] and Sreenivasan and White [7] have studied the drag reduction effect in dilute polymer solutions, and Hoyt [8] and Kawaguchi et al. [9] have also reported on this effect in surfactant solutions; however, the use of such liquids is limited because of environmental concerns. Hasegawa et al. [10] and Ushida et al. [11,12] have measured the pressure drops for water, glycerol, and silicone oils passing through micro-orifices and reported lower pressure drops than the predictions of the Navier–Stokes equations; a drag reduction effect was found in Newtonian fluids. Against this background, the drag reduction effect for mixed nanobubble water and aqueous solution of glycerol, passed through a micro-orifice or capillary, was investigated in the present research.

2. Experimental methods

2.1. Micro-orifices

Optical pinholes (Sigma Koki Co., Ltd.; PA-5–PA-100) were used as micro-orifices, for which diameter, D, ranged from 5 μm to 100 μm. The thickness, L, of all micro-orifices was 20 μm. Fig. 1a and b shows close-up images of a micro-orifice (D = 50 μm) as observed by scanning electron microscopy. The front and back sides of the orifice had different shapes, as was seen in previous research [10–12], but this difference in shape had no effect on the flow behavior.

2.2. Experimental apparatus

Fig. 2 shows an overview of the experimental apparatus used in the present research. The basic structure of the apparatus is the same as that used by Hasegawa et al. [10] and Ushida et al. [11,12]. A test liquid was charged in a syringe pump (Furue Science

* Corresponding author. Address: 8050-2 Ikarashi, Nishi-ku, Niigata-shi, Niigata 950-2181, Japan. Tel./fax: +81 25 262 6712.
E-mail address: akiomiushida@gs.niigata-u.ac.jp (A. Ushida).

0894-1777/$ - see front matter © 2012 Published by Elsevier Inc.
doi:10.1016/j.expthermflusci.2012.01.008

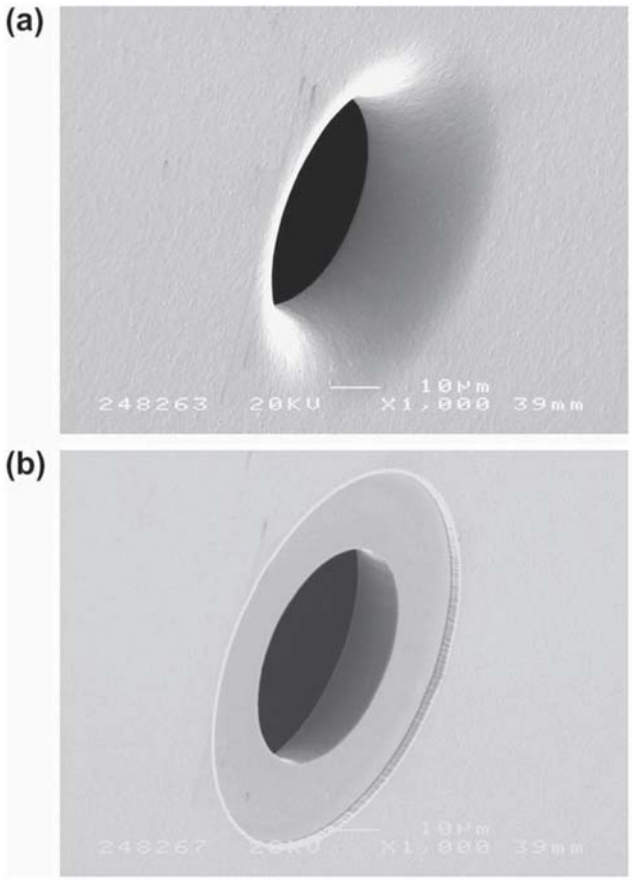

Fig. 1. Schematic diagram of micro-orifice (diameter: 50 μm): (a) front side, and (b) back side.

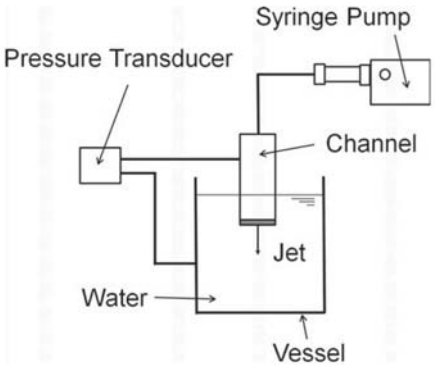

Fig. 2. Experimental apparatus for measuring pressure drop.

Co., Ltd.; JP-H1) and then fed into a channel at a constant flow rate, Q. A micro-orifice was placed at the end of the channel, and the liquid was passed as a jet through the micro-orifice. Pressure ports were built into the acrylic channel (inner diameter; 25 mm, length; 180 mm) and acrylic vessel. The difference in pressure was measured as pressure drop, Δp, by using a pressure transducer (Tsukasa Sokken Co., Ltd.; SPD-12).

2.3. Test liquids

Test liquids used in this research were as follows: an aqueous solution containing 1.0 vol.% nanobubbles (hereinafter called NB water) and ion-exchanged water (ADVANTC Co., Ltd.; GSR-200) (hereinafter simply called water). In addition, aqueous solution of glycerol and mixed nanobubble glycerol aqueous solution were used (hereinafter called glycerol and NB/glycerol mixture). The nanobubble liquid was prepared with a nanobubble generator (Daiko Engineering Co., Ltd.; HANDS-S-10) by means of a high-swirl flow (Fig. 3a). The resulting mixture contained 1.0 vol.% nanobubbles, as determined on a nanoparticle analyzer (Quantum Design Japan Co., Ltd.; NanoSight LM1-HS); furthermore, the nanobubble diameter, also measured on the nanoparticle analyzer, was approximately

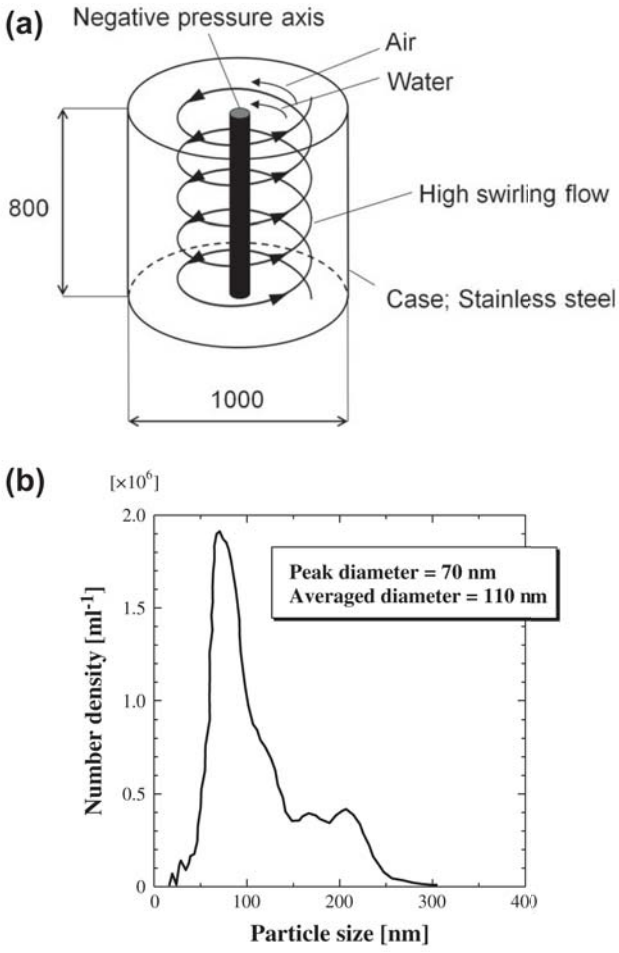

Fig. 3. Schematic diagrams of (a) mixed air/water flow, and (b) number density plotted against particle size of nanobubbles.

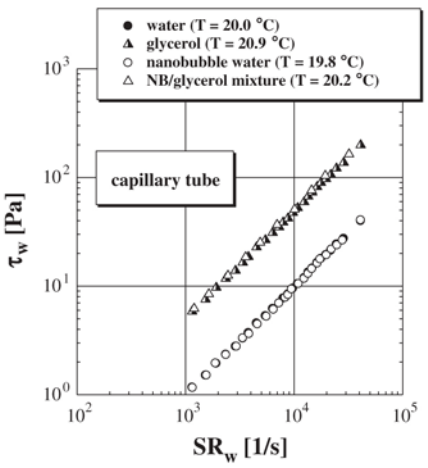

Fig. 4. Measurement of viscosity of test liquids.

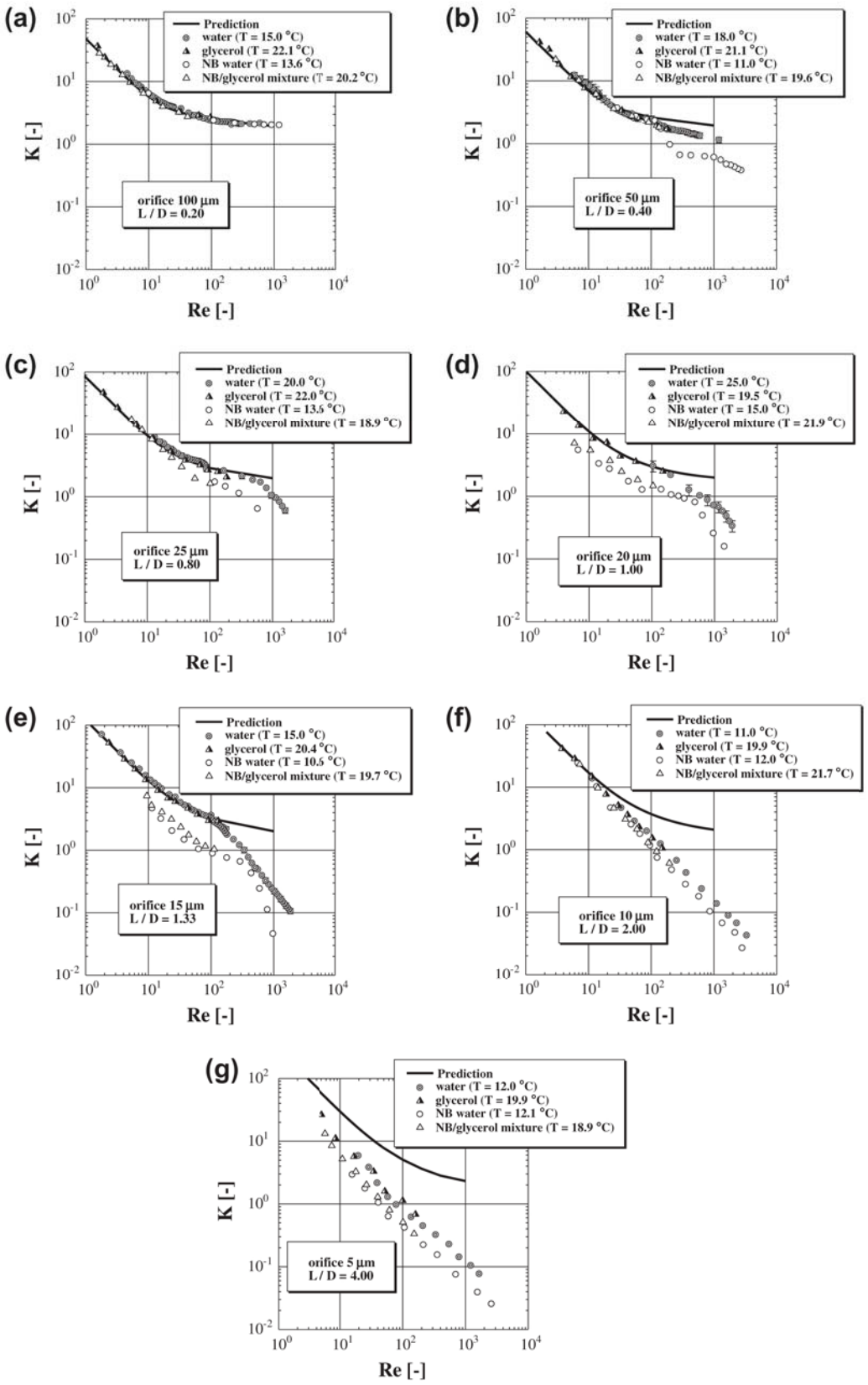

Fig. 5. Dimensionless pressure drops, *K*, plotted against Reynolds number, *Re*, for orifices with diameters of (a) 100 μm, (b) 50 μm, (c) 25 μm, (d) 20 μm, (e) 15 μm, (f) 10 μm, and (g) 5 μm.

110 nm (peak diameter was 70 nm) (Fig. 3b). Zeta potential of NB water was about -17.1 mV at pH = 7.1. This value was the same for the previous result [13,14]. Additionally, the density, ρ, of nanobubble mixture was measured on the Baumé scale, and found to be 0.992 times the density of water and glycerol (=1.0 × 10^3 kg/m^3). This density was averaged value by numerous measurements

Please cite this article in press as: A. Ushida et al., Drag reduction effect of nanobubble mixture flows through micro-orifices and capillaries, Exp. Therm. Fluid Sci. (2012), doi:10.1016/j.expthermflusci.2012.01.008

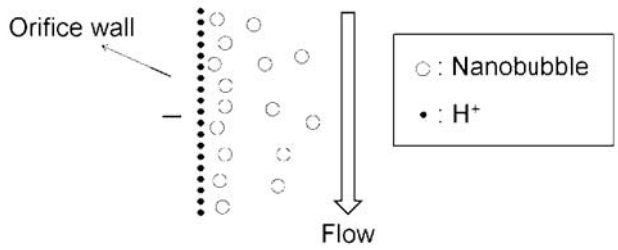

Fig. 6. Schematic image of interface between electric double layer and nanobubbles.

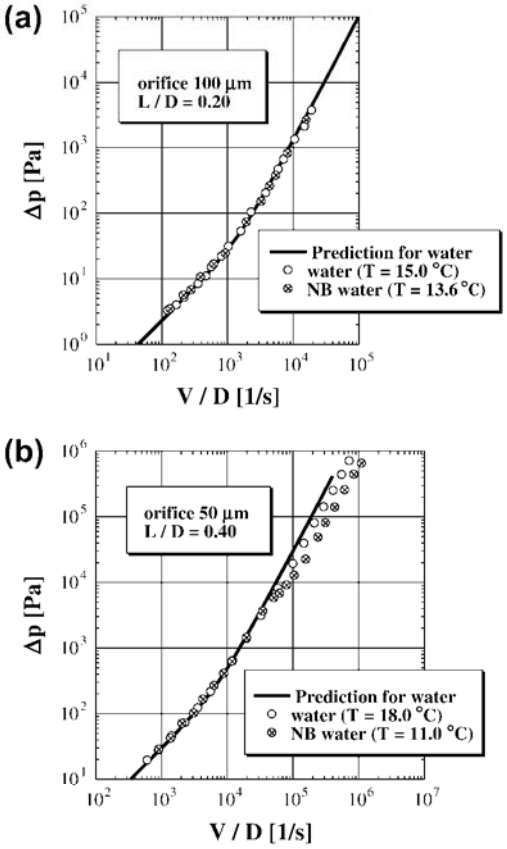

Fig. 7. Pressure drops, Δp, versus strain rate, V/D, for (a) 100 μm, and (b) 50 μm.

in the temperature ranges 5–30 °C. Viscosity, μ, was measured on a capillary viscometer (inner diameter: 1.0 mm). Fig. 4 shows shear stress plotted against shear rate, and viscosity, μ, is given by

$$\tau_w = \mu(SR_w), \tag{1}$$

where τ_w is the shear stress at the wall and SR_w is the shear rate. The viscosity of NB water was found to be the same as the viscosity of water ($\mu = 1.0 \times 10^{-3}$ Pa s). The viscosity of glycerol and NB/glycerol mixture were 5 times greater than those of water ($\mu = 5.0 \times 10^{-3}$ Pa s). Here, the measured pressure drop, Δp, is expressed as a dimensionless pressure drop, $K(=2\Delta p/\rho V^2)$, and the Reynolds number is given by $Re(=\rho VD/\mu$, where, V is the mean velocity$(=4Q/\pi D^2)$). The test liquid temperatures are shown in the figures along with the results.

3. Experimental results

Fig. 5a–g shows the results for water, NB water, glycerol, and NB/glycerol mixture passed through orifices of 100–5 μm in diameter. The vertical axis shows K, and the horizontal axis shows Re. For comparison, the predictions from the Navier–Stokes equations [10] are also shown. When using an orifice of 100 μm in diameter, the experimental results for all test liquids agreed with the predictions from the Navier–Stokes equations (Fig. 5a). However, when using orifices of 50–5 μm in diameter, the resultant pressure drops for mixed nanobubble liquids (NB water and NB/glycerol mixture) were lower than those for water and glycerol (Fig. 5b–g). Drag reduction was observed for the nanobubble mixture.

4. Discussion

4.1. Flow of NB water and NB/glycerol mixture

Pressure drops were measured when NB water and NB/glycerol mixture having an average bubble diameter of approximately 110 nm were passed through micro-orifices of 100–5 μm in diameter. The experimentally measured pressure drops for NB water were lower than those for water, and NB/glycerol mixture had lower pressure drops for glycerol, when orifices of $\leqslant$50 μm in diameter were used (Fig. 5b–g). In previous research, Hasegawa et al. [10] and Ushida et al. [11] reported on the possibility that water flow through a micro-orifice is elastic, but in the case of NB water containing only air, it is not thought that the results can be explained in terms of elasticity. In research employing Re values similar to those in this research, Ushida et al. [12] noted that surfactant molecules behaved like polymer chains as a result of electrical interactions, and were therefore able to exhibit a phenomenon similar to viscoelasticity. The present results are similar to the previous results [12] in terms of electrical interactions, but we consider the results from a slightly different perspective. In general, solid wall surfaces carry negative charge in water; this is widely known as an electrical double layer [15–18]. In addition, microbubbles and nanobubbles have also been found to carry negative charge in aqueous solution [19]. Fig. 6 shows a schematic diagram of nanobubble flow near an orifice wall. The liquid around the orifice carries positive charge (H^+) due to the electrical double layer. Thus, in electrical terms, the bubbles carrying negative charge can be regarded as a flow that passes a positively charged wall surface. In that case, an electrical attraction would occur, and the bubbles would thus adhere to the wall surface. Then, a gas phase would form near the surface of the orifice wall, and the NB water would flow along this gas phase. Owing to the presence of this gas phase, a wall slip phenomenon would occur between the wall surface and the liquid surface. Furthermore, the effect should become more pronounced as the thickness ratio (L/D) is increased, that is, as the wall surface along which the liquid flows becomes longer relative to the orifice diameter. It thus follows that the electrical effect increases as the effect of the wall surface increases, and this is consistent with the results shown in Fig. 5b–g. In addition, the drag reduction effect was not seen when using an orifice of 100 μm in diameter (Fig. 5a). This is attributed to the thickness of the electrical double layer being approximately 1.0 μm [20,21] and the region subjected to the electrical effect thus being small relative to the size of the orifice (the larger thickness ratio was, the bigger electrical effect was). Also, the experimental results were contributed to strain rate. Fig. 7a and b shows pressure drops, Δp, plotted against strain rate, $V/D(=4Q/\pi D^3)$. In Fig. 7b, the reduction occurred for $V/D > 5.0 \times 10^4$/s. However, in Fig. 7a, strain rate ranges from 1.0×10^2/s to 1.0×10^4/s. Thus, it was found that the reduction did not appear.

4.2. Direct numerical simulation of slip condition at wall

To examine the drag reduction due to wall slip in further detail, direct numerical simulation was carried out for orifice flows under

Please cite this article in press as: A. Ushida et al., Drag reduction effect of nanobubble mixture flows through micro-orifices and capillaries, Exp. Therm. Fluid Sci. (2012), doi:10.1016/j.expthermflusci.2012.01.008

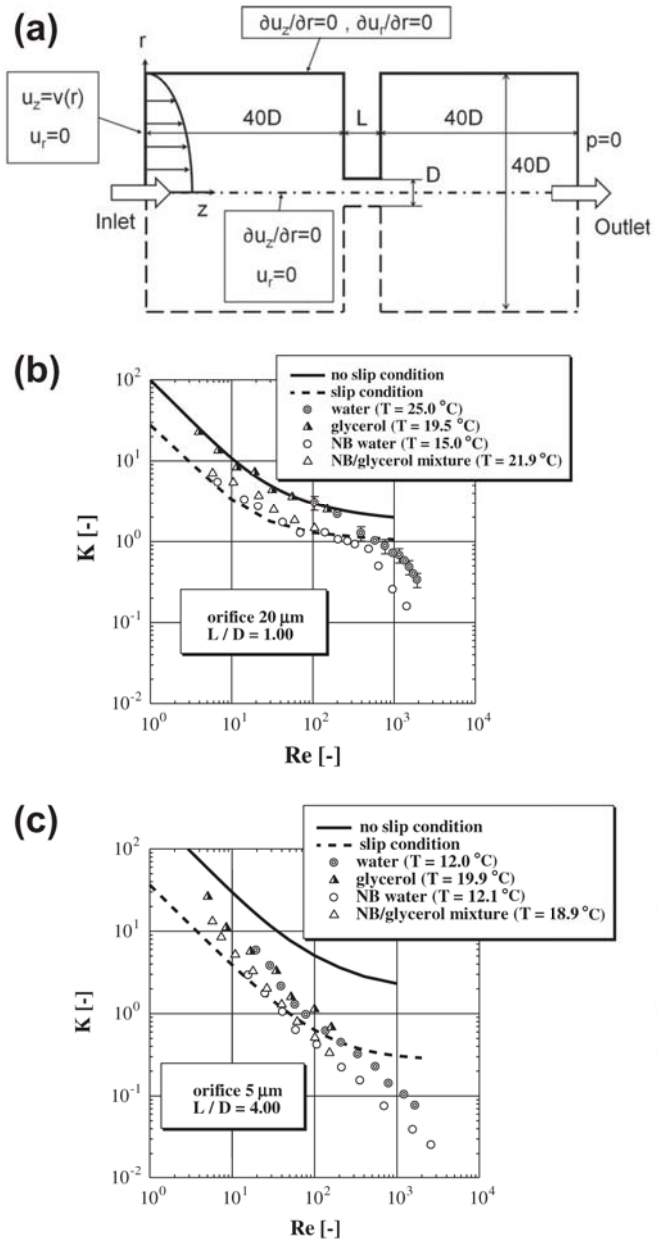

Fig. 8. (a) Schematic diagram of numerical model and boundary conditions, and numerical results for slip condition and a comparison between the present results for (b) 20 μm, and (c) 5 μm.

slip conditions. The two-dimensional cylindrical dimensionless Navier–Stokes equations are

$$\frac{\partial u_z^*}{\partial t^*} + u_r^* \frac{\partial u_z^*}{\partial r^*} + u_z^* \frac{\partial u_z^*}{\partial z^*} = -\frac{\partial p^*}{\partial z^*} + \frac{1}{Re}\left\{\frac{1}{r^*}\frac{\partial}{\partial r^*}\left(r^* \frac{\partial u_z^*}{\partial r^*}\right) + \frac{\partial^2 u_z^*}{\partial z^* \partial z^*}\right\} \quad (2)$$

and

$$\frac{\partial u_r^*}{\partial t^*} + u_r^* \frac{\partial u_r^*}{\partial r^*} + u_z^* \frac{\partial u_r^*}{\partial z^*} = -\frac{\partial p^*}{\partial r^*} + \frac{1}{Re}\left[\frac{\partial}{\partial r^*}\left\{\frac{1}{r^*}\frac{\partial}{\partial r^*}(r^* u_r^*)\right\} + \frac{\partial^2 u_r^*}{\partial z^* \partial z^*}\right], \quad (3)$$

where the direction is ignored because the θ direction does not change. The finite volume method is adopted for a Newtonian fluid passing through an orifice, in which the velocity and pressure are expressed on a staggered grid in a two-dimensional cylindrical coordinate system. Velocity and pressure are coupled by the SIMPLE method. The convective term is discretized by the first-order upwind finite difference method, and the viscous term is discretized by the second-order central difference method. Fig. 8a shows the numerical model. The diameter of the channel upstream and downstream of the orifice are 40*D*, the upstream and downstream lengths are 40*D*. The following boundary conditions are adopted: (a) Poiseuille flow exists at the inlet boundary; (b) the pressure and velocity in the radial direction are zero at the outlet boundary; (c) the radial component of the velocity is zero along the center line; and (d) all velocity gradients are zero at the wall (slip conditions). Fig. 8b shows the pressure drop plotted versus Reynolds number for the present numerical results (broken line) and the experimental results for 20 μm, along with the previous results for water [10]. The calculated predictions nearly agree with the experimental results for an orifice of 20 μm in diameter. However, the predicted

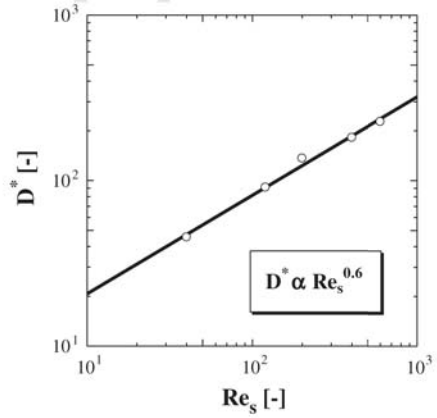

Fig. 9. D^* plotted against Re_s in the ranges from 5 μm to 25 μm.

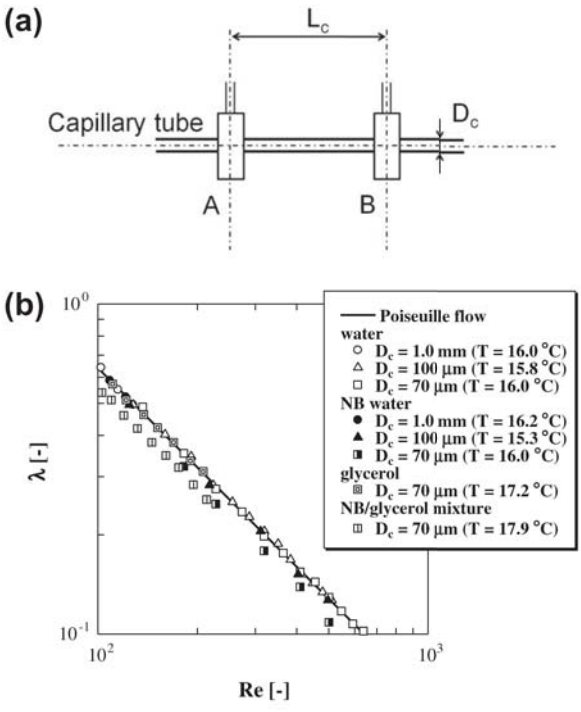

Fig. 10. (a) Experimental apparatus, and (b) λ versus Re for capillary flows.

Please cite this article in press as: A. Ushida et al., Drag reduction effect of nanobubble mixture flows through micro-orifices and capillaries, Exp. Therm. Fluid Sci. (2012), doi:10.1016/j.expthermflusci.2012.01.008

pressure drop was less than that observed in the experiment at $Re > 400$. Fig. 8c shows the experimental and numerical results for 5 μm in diameter. In the case of 5 μm, the experimental results were less than the present (slip) prediction at $Re > 20$. Additionally, Fig. 9 shows diameter ratio, D^*, versus any Reynolds number in which the resultant pressure drops were smaller than the present predictions, Re_s. Here, diameter ratio was expressed as the ratio of orifice size to bubble's particle size (≈110 nm). It was found that there were power relation between D^* and Re_s. Furthermore, Hasegawa et al. [22–24] have reported the possibility of viscoelastic stress in orifice flows. However, it was not reasonable to support that the present results were caused by nanobubble mixtures.

5. Frictional coefficient of capillary

Drag reduction was found in orifice flow of nanobubble mixture and explained in terms of wall slip. Therefore, three types of capillaries were employed to investigate the effects of slip. The stainless steel capillaries were 1.0 mm, 100 μm, and 70 μm in inner diameter. The frictional coefficient λ was measured for water, glycerol, NB water, and NB/glycerol mixture. Fig. 10a shows the experimental setup. Pressure drops were measured, and λ is given by

$$\lambda = \frac{2\Delta p}{\rho V^2}\frac{D_c}{L_c}, \tag{4}$$

where D_c is the diameter of the capillary and L_c(≈250 mm) is the distance between two pressure ports. The syringe pump and pressure transducer used in this experiment were the same as in the orifice flow experiments. Fig. 10b shows the experimental results for λ plotted against Re. All λ values agreed with the prediction for Poiseuille flow except for nanobubble mixtures in the capillary with inner diameter of 70 μm; in that case, the discrepancy was less than 10%. It was found that the properties of the liquids (*e.g.*, elasticity) were not affected in the case of capillary flow. In fact, the reduction (D_c = 70 μm, NB water and NB/glycerol mixture) was caused by wall slip. These results strongly suggest that nanobubble mixture exhibits a drag reduction effect.

6. Conclusion

In this research, pressure drops were measured for mixed nanobubble water and glycerol passed through a micro-orifice or capillary, and through comparison with water and glycerol, the following results were obtained.

I. For an orifice of 100 μm in diameter, the pressure drop was the same for NB water and NB/glycerol mixture as for water and glycerol, respectively. However, when using orifices of ⩽50 μm in diameter, the pressure drop in the case of mixed nanobubble was lower than that in the case of without nanobubble, and a drag reduction effect was observed.

II. The drag reduction was explained by interface phenomena. The nanobubbles adhered to the wall surface, forming a gas phase, which resulted in wall slip. Through a comparison between numerical and experimental results, the results for nanobubbles were found to be consistent with wall slip.

III. In capillary flow (inner diameter: 70 μm), the frictional coefficient for NB water and NB/glycerol mixture was less than that for Poiseuille flow.

Acknowledgements

We wish to thank Mr. Ryuichi Kayaba, Mr. Naoyuki Takahashi, Mr. Takayuki Aoike, and Mr. Shotaro Murao for technical assistance in many experiments and numerical analyses. We also thank Mr. Shouta Kudou, Mr. Masato Kawami, Dr. Keiko Amaki and Prof. Shinji Toga for help with the research and their fruitful comments. In addition, we thank Dr. Kazuhiro Maeshima for English correction.

References

[1] Y. Kodama, A. Kakugawa, T. Takahashi, H. Yamaguchi, Experimental study on microbubbles and their applicability to ships for skin friction reduction, International Journal of Heat and Fluid Flow 21 (2000) 582–588.
[2] H. Kato, T. Iwashina, M. Miyanaga, H. Yamaguchi, Effect of microbubbles on the structure of turbulence in a turbulent boundary layer, Journal of Marine Science and Technology 4 (1999) 155–162.
[3] S. Liu, Q. Wang, H. Ma, P. Hung, J. Li, T. Kikuchi, Effect of micro-bubbles on coagulation flotation process of dyeing wastewater, Separation and Purification Technology 71 (2010) 337–346.
[4] S. Liu, Q. Wang, T. Sun, C. Wu, Y. Shi, The effect of different types of microbubble on the performance of the coagulation flotation process for coke waste water, Chemical Technology and Biotechnology (2011) 1–10 (doi:10.1002/jctb.2698).
[5] Z. Wu, H. Chen, Y. Dong, H. Mao, J. Sun, S. Chen, V.S.J. Craig, J. Hu, Cleaning using nanobubbles: defouling by electrochemical generation of bubbles, Journal of Colloid and Interface Science 328 (2008) 10–14.
[6] E.D. Burger, W.R. Munk, H.A. Wahl, Flow increase in the trans Alaska pipeline through use of a polymeric drag-reducing additive, Journal of Petroleum Technology 34 (1982) 377–386.
[7] K.R. Sreenivasan, C.M. White, The onset of drag reduction by dilute polymer additives, and the maximum drag reduction asymptote, Journal of Fluid Mechanics 409 (2000) 149–161.
[8] J.W. Hoyt, Drag reduction by polymers and surfactants, AIAA Progress an Astronautics and Aeronautics 123 (1990) 413–432.
[9] Y. Kawaguchi, F.C. Li, B. Yu, J.J. Wei, Turbulent drag reduction with surfactant additives – basic research and application to an air conditioning system, New Trends in Fluid Mechanics Research 1 (2009) 29–36.
[10] T. Hasegawa, A. Ushida, T. Narumi, Huge reduction in pressure drop of water, glycerol/water mixture, and aqueous solution of polyethylene oxide in high speed flows through micro-orifices, Physics of Fluids 21 (2009) 052002.
[11] A. Ushida, T. Hasegawa, T. Narumi, Drag reduction for liquid flow through micro-apertures, Journal of Non-Newtonian Fluid Mechanics 165 (2010) 1516–1524.
[12] A. Ushida, T. Hasegawa, S. Kudou, M. Kawami, H. Uchiyama, T. Narumi, Flow properties for several types of liquid flows through micro-orifices, Journal of Fluid Science and Technology 6 (2011) 802–811.
[13] J.Y. Kim, M.G. Song, J.D. Kim, Zeta potential of nanobubbles generated by ultrasonication in aqueous alkyl polyglycoside solutions, Journal of Colloid and Interface Science 223 (2000) 285–291.
[14] F. Jin, J. Li, X. Ye, C. Wu, Effects of pH and ionic strength on the stability of nanobubbles in aqueous solutions of α-cyclodextrin, Journal of Physical Chemistry B 111 (2007) 11745–11749.
[15] D.C. Grahame, The electrical double layer and the theory of electrocapillarity, Chemical Review 41 (1947) 441–501.
[16] M. Srinivas, E.G. Hermann, Molecular organization of surfactants at solid-liquid interfaces, Science 270 (1995) 1480–1482.
[17] C. Yang, D. Li, Electrokinetic effects on pressure-driven liquid flows in rectangular microchannels, Journal of Colloid and Interface Science 194 (1997) 95–107.
[18] M.V. Fedorov, A.A. Kornyshev, Ionic liquid near a charged wall: structure and capacitance of electrical double layer, Journal of Physical Chemistry B 112 (2008) 11868–11872.
[19] S.H. Cho, J.Y. Kim, J.H. Chun, J.D. Kim, Ultrasonic formation of nanobubbles and their zeta-potentials in aqueous electrolyte and surfactant solutions, Colloids and Surfaces A: Physicochemical and Engineering Aspects 269 (2005) 28–34.
[20] D. Li, Electrokinetics in microfluidics, vol. 2, Elsevier, 2004. pp. 8–27.
[21] G. Hu, D. Li, Multiscale phenomena in microfluidics and nanofluidics, Chemical Engineering Science 62 (2007) 3443–3454.
[22] T. Hasegawa, T. Iwaida, Experiments on elongational flow of dilute polymer solutions: Part II: velocity field for the flow through small apertures, Journal of Non-Newtonian Fluid Mechanics 15 (1984) 279–307.
[23] T. Hasegawa, H. Asama, T. Narumi, A simple method for measuring elastic stresses by jet thrust and some characteristics of tube flows, Nihon Reoroji Gakkaishi 31 (2003) 243–252.
[24] T. Hasegawa, H. Watanabe, T. Sato, T. Watanabe, M. Takahashi, T. Narumi, T. Carlos, Anomalous reduction in thrust/reaction of water jets issuing from microapertures, Physics of Fluids 19 (2007) 053102.